Gold Nanoparticle Functionalized Artificial Nacre: Facile *in Situ* Growth of Nanoparticles on Montmorillonite Nanosheets, Self-Assembly, and Their Multiple Properties

Hong-Bin Yao,[†] Li-Bo Mao,[†] You-Xian Yan, Huai-Ping Cong, Xuan Lei, and Shu-Hong Yu*

Division of Nanomaterials and Chemistry, Hefei National Laboratory for Physical Sciences at the Microscale, Department of Chemistry, the National Synchrotron Radiation Laboratory, University of Science and Technology of China, Hefei, Anhui 230026, P. R. China. [†]These authors contributed equally to this work.

ABSTRACT Artificial nacre based on clay nanosheets have been emerging as a new generation of bioinspired materials due to their super mechanical, fire-retardant, heat-shield, and gas barrier properties. Functional design in artificial nacre is highly demanded to further broaden the applications of these promising bioinspired materials. However, there is rarely a report on the functionalization of artificial nacre at present possibly due to the lack of a feasible strategy to introduce functional components in nacre-like materials without weakening other properties. In this study, we report a feasible method to fabricate artificial nacre-like functional hybrid films by using Au nanoparticle (NP) modified natural clay montmorillonite (MTM) nanosheets as efficient two-dimensional building blocks. First, Au NPs-chitosan-MTM hybrid nanosheets were prepared and homogeneously dispersed in deionized water by the facile *in situ* growth of Au NPs on chitosan-MTM nanosheets. Then, the obtained Au NPs-chitosan-MTM hybrid nanosheet suspension can be sprayed or vacuum filtrated to form nacre-like layered hybrid nanocoatings or free-standing hybrid films, respectively. Finally, as-fabricated artificial nacre nanocoatings or hybrid films have been demonstrated to behave with surface enhanced Raman scattering (SERS), catalytic, and photothermal conversion properties indicating the successful functionalization of artificial nacre by introducing Au NPs.

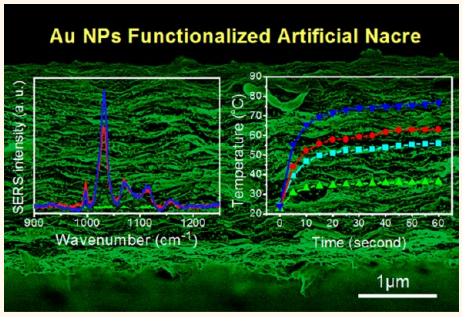

KEYWORDS: nacre-like · multifunctional films · Au NPs-chitosan-MTM · nanocomposite · SERS · photothermal conversion

Nacre, an inner layer of mollusk shells, is the main constituent of the protective armor system with a unique combination properties that include lightweight, strength, stiffness, and toughness.[1,2] Surprisingly, nacre is only composed of a large fraction of biominerals and a small fraction of organic biopolymers, and both of these compositions are weak and fragile.[3] Because of the great advantages provided by nacre compared with conventional artificial materials, it has been one of the most extensively attractive biological models to inspire the design and fabrication of artificial materials with high mechanical performance.[4−6] The microstructure study shows that nacre owns a perfect `brick-and-mortar' arrangement of highly aligned inorganic aragonite microplatelets surrounded by a protein matrix, serving as glue between the platelets.[4,7] It is commonly considered that the `brick-and-mortar' microstructure of nacre is the main model that plays an important role in its excellent mechanical properties.[3,7,8]

By mimicking the `brick-and-mortar' layered microstructures of nacre, a series of nacre-like artificial materials have been produced by the assembly of various artificial inorganic building blocks with polymers.[9,10] The clay nanosheets,[11] ceramic nanoparticles,[12] layered double hydroxide platelets,[13] and biominerals[14] can be assembled with polymers to form layered microstructures through feasible assembly techniques. In particular, the natural clay montmorillonite (MTM) nanosheets are ideal two-dimensional inorganic building blocks to fabricate layered structural artificial nacre. For example, layer by layer deposition of MTM nanosheets and polymers generated nacre-like hybrid films with high tensile strength;[11,15,16] MTM nanosheets were aligned into lamellar structures by electrophoretic deposition to construct a nacre-like hybrid film with following post-treatment;[17,18] layered MTM-polyimide hybrid films were prepared *via* the centrifugal deposition process;[19] the self-assembly

* Address correspondence to shyu@ustc.edu.cn.

Received for review July 1, 2012 and accepted August 21, 2012.

Published online August 21, 2012
10.1021/nn3029315

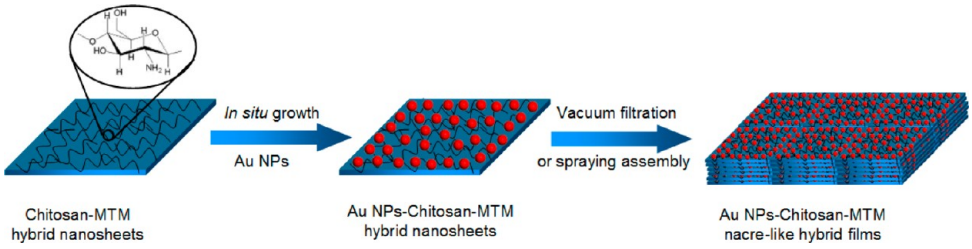

Figure 1. Schematic illustration of proposed fabrication procedure of artificial nacre-like functional Au NPs-chitosan-MTM hybrid films.

process of MTM-polymer hybrid building blocks was also used to build the nacre-like hybrid film.[20−22]

With the development of assembly techniques of MTM nanosheets with polymers, especially, the self-assembly process of MTM and the chitosan biopolymer,[22] the facile and large area fabrication of artificial nacre is easily achieved. Because of the nacre-like layered microstructures inside, these obtained hybrid films behaved with interesting fire retardant,[22] heat-shield,[20,21] and gas-barrier properties.[23,24] Furthermore, the tensile strength of the obtained artificial nacre-like clay−polymer hybrid films is better than that of conventional clay−polymer nanocomposites due to the optimized applied load transfer from polymer to clay nanosheets. The functionalization of MTM-polymer artificial nacre *via* incorporation of nanocomponents is highly demanded for further broadening the applications of these novel bioinspired materials. However, there is rarely a report on the functional design of artificial nacre or the preparation of multifunctional artificial nacre, possibly due to the lack of a feasible strategy to introduce proper functional components in nacre-like materials without weakening other properties.

For introducing functionalities into artificially nacre-like layered structural hybrid films, nanoparticles are efficient components due to their small sizes, facile assemblies, special properties and wide applications in traditional functional nanocomposites.[25−29] Previous Au NP based nanocomposites showed potential applications in the fields of advanced microelectronics, nonlinear optics, electrochemical sensors, and bioanalysis.[30−32] Thus, Au NPs are highly expected to be embedded in the layered structures of artificial nacre in order to endow functionalities. Although previously Au NPs have been assembled with a polyelectrolyte *via* layer by layer (LBL) deposition to prepare functional layered structural hybrid films with suitable mechanical properties,[25,33−35] this LBL assembly process is time-consuming and hard to scale up for practical applications.

Herein, we propose a novel strategy to fabricate Au NPs-chitosan-MTM artificial nacre through *in situ* growth and decoration of Au NPs on chitosan-MTM nanosheets and subsequent self-assembly of as-synthesized Au NPs-chitosan-MTM hybrid nanosheets. Our proposed fabrication strategy can realize quick and large scale production of functional artificial nacre-like hybrid materials. In this designed approach, the green synthesis of Au NPs-chitosan-MTM hybrid nanosheets was first achieved. The chitosan molecules adsorbed on MTM nanosheets were used as cheating, reducing/stabilizing agents to localize Au NPs on hybrid nanosheets. The chitosan molecules absorbed on MTM hybrid nanosheets played a crucial role in the *in situ* growth of Au NPs, which is similar to the previous report on the chitosan mediated-synthesis of Au NPs.[36−38] Besides chitosan molecules on hybrid nanosheets, we also added sodium citrate in the synthetic system as reducing/stabilizing agents to control the growth of Au NPs which further improved the quality (size and distribution homogeneity) of Au NPs attached on the hybrid nanosheets. Exceeding the green synthesis procedure, the synthesized Au NPs-chitosan-MTM hybrid nanosheets can be dispersed into a glacial acetic acid aqueous solution enabling the feasibility of their self-assembly to form functional nacre-like layered coatings and freestanding hybrid films. This assembly process to generate the artificial nacre-like Au NPs-chitosan-MTM hybrid materials has not been reported in previous work on the chitosan-mediated synthesis of Au NPs.[36,37] More importantly, because of the nacre-like layered microstructure and the incorporation of Au NPs, the present Au NPs-chitosan-MTM hybrid freestanding films not only display high tensile strength but also possess multiple properties such as SERS, catalysis, and photothermal activities.

RESULTS AND DISCUSSION

Au NPs-Chitosan-MTM Artificial Nacre-like Hybrid Coating or Film Fabrication Route. Our designed fabrication procedure involves the green synthesis of highly dispersible Au NPs-chitosan-MTM hybrid nanosheets and self-assembly of as-syntheiszed Au NPs-chitosan-MTM hybrid nanosheets. The whole fabrication procedure of an artificial nacre-like layered structural functional Au NPs-chitosan-MTM hybrid coatings or films is depicted in Figure 1. First, Au NPs-chitosan-MTM functional building blocks were synthesized by taking advantage of *in situ* growth of Au NPs on chitosan-MTM hybrid nanosheets *via* a one-step reaction. The synthesized Au NPs-chitosan-MTM hybrid nanosheet red gel was collected by centrifugation and then easily dispersed in distilled water forming a homogeneous red

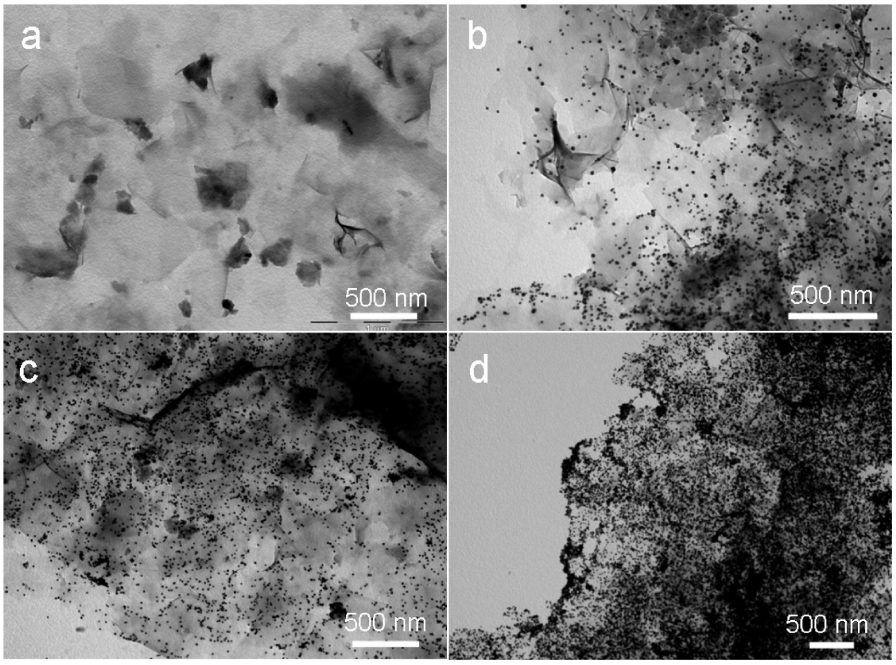

Figure 2. TEM images of chitosan-MTM and Au NPs-chitosan-MTM hybrid nanosheets. (a) Original chitosan-MTM hybrid nanosheets. (b, c, and d) Au NPs-chitosan-MTM hybrid nanosheets generated in the reaction system of $C_{chloroauric\ acid}$: $C_{chitosan\text{-}MTM}$ = 1:25, 2:25, and 4:25, respectively.

suspension. Finally, through the spraying or vacuum filtration induced self-assembly of the Au NPs-chitosan-MTM hybrid nanosheets aqueous suspension, artificial nacre-like functional coatings or freestanding hybrid films were fabricated.

***In Situ* Growth and Decoration of Au NPs on Chitosan-MTM Hybrid Nanosheets.** By utilizing chitosan molecules on MTM nanosheets as chelating agents and stabilizers, Au NPs were decorated on the chitosan-MTM hybrid nanosheets *via* a one-step refluxing process. In the synthetic procedure, $AuCl_4^-$ ions were first mixed with a chitosan-MTM hybrid nanosheet aqueous suspension and stirred sufficiently to guarantee the adsorption of $AuCl_4^-$ on nanosheets by the chelating role of chitosan. Then, sodium citrate was added into the mixture as a reduction agent and surfactant to promote the growth of Au NPs and control the particle sizes. After refluxing, Au NPs were *in situ* formed on chitosan-MTM hybrid nanosheets under the reducing and stabilizing role of citrate and chitosan. Figure 2 a and b show the transmission electron microscopy (TEM) images of chitosan-MTM hybrid nanosheets before and after *in situ* growth of Au NPs respectively. Obviously, many homogeneous nanoparticles appeared on chitosan-MTM hybrid nanosheets after the reaction compared with original chitosan-MTM hybrid nanosheets. Furthermore, the area beside the nanosheets in the TEM image is blank without the appearance of any individual nanoparticles, which indicates that all the formed Au NPs were absorbed on the chitosan-MTM hybrid nanosheets. The successful decoration of Au NPs on chitosan-MTM hybrid nanosheets was further confirmed by scanning electron microscopy (SEM), and the particle size of Au NPs was measured as ~20 nm (Supporting Information Figure S1).

Our designed synthesis method is similar to the green synthesis of metal nanoparticles by using protein, polysaccharides, and nucleic acids as reducing/stabilizing agents,[39−42] especially the chitosan-mediated synthesis of Au NPs.[36−38] However, it is worth noting that in our reaction system we achieved good control of particle size, distribution homogeneity, and adhesion with hybrid nanosheets by adding sodium citrate in the reaction system. The TEM images of the Au NPs-chitosan-MTM hybrid nanosheets synthesized without adding sodium citrate (control experiment) show that the amount of Au NPs absorbed on hybrid nanosheets largely decreased and that many individual small Au NPs nanoparticles appeared outside the nanosheets and the sizes of obtained Au NPs were inhomogeneous (Figure S2). The citrates were usually used as negative surfactants for the synthesis of Au NPs which can control the particle size well and make the synthesized Au NPs behave with a negative charge endowing them with strong adhesion with the positively charged chitosan molecules on MTM nanosheets. Compared with the previously reported chitosan-mediated synthesis of Au NPs,[36−38] we can achieve better size control of Au NPs, stronger adhesion, and a higher adsorption amount of Au NPs on substrates *via* using citrate as the stabilizer besides chitosan.

In addition, through varying the concentration ratio of the chitosan-MTM hybrid nanosheet and chloroauric

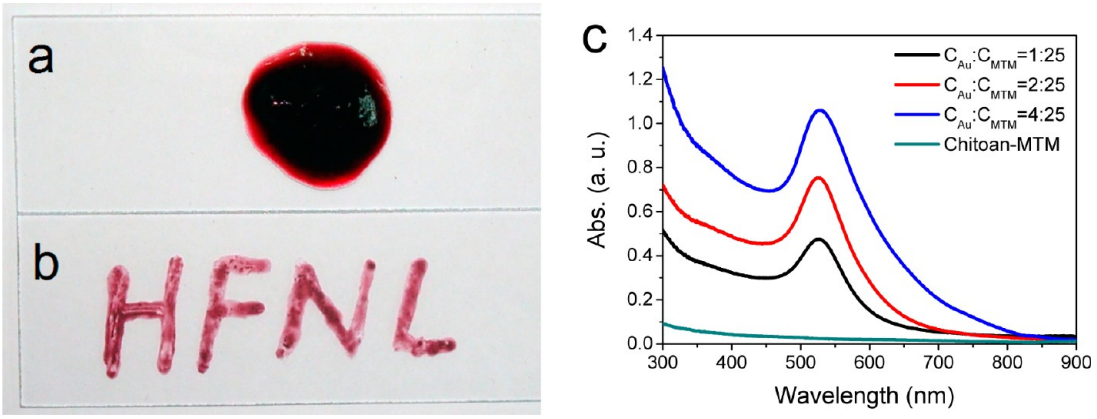

Figure 3. (a) Photograph of collected Au NPs-chitosan-MTM hybrid glue. (b) Photograph of "HFNL" pattern painted on glass substrate by using as-prepared Au NPs-chitosan-MTM hybrid glue. (c) UV−vis spectra of chitoan-MTM hybrid nanosheet suspension and Au NPs-chitosan-MTM hybrid nanosheet suspension with different Au NP densities on the MTM nanosheets.

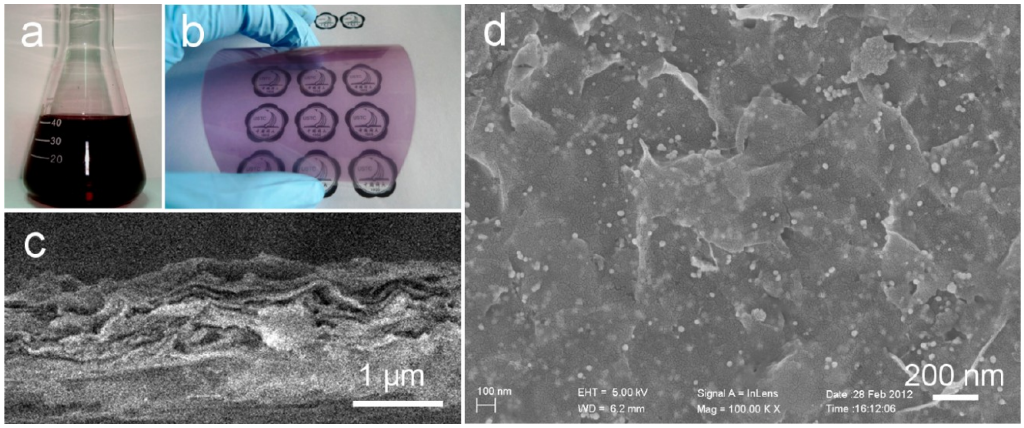

Figure 4. (a) Photograph of aqueous suspension of Au NPs-chitosan-MTM hybrid nanosheets. (b) Photograph of flexible Au NPs-chitosan-MTM hybrid nanosheets-PET film. (c) Cross-sectional SEM image of Au NPs-chitosan-MTM hybrid nanosheets coating on PET substrate. (d) SEM image of the surface of Au NPs-chitosan-MTM hybrid nanosheets coating on PET film.

acid in suspension, the distribution density of Au NPs on chitosan-MTM nanosheets can be easily tuned. As confirmed by TEM images (Figure 2b−d), as the concentration ratio of the chloroauric acid solution and chitosan-MTM hybrid nanosheets in suspension gradually increased, the distribution density of Au NPs on the chitosan-MTM hybrid nanosheets increased. In particular, when the concentration ratio of chloroauric acid and the chitosan-MTM hybrid nanosheets reaches 4:25, the formed Au NPs almost covered the whole surface of the chitosan-MTM hybrid nanosheets (Figure 2d).

The synthesized Au NPs-chitosan-MTM hybrid nanosheets were collected as a red glue-like substance through centrifugation (Figure 3a). The obtained Au NPs-chitosan-MTM red glue displayed high adhesion with each other and to the glass substrate due to the linking role of chitosan molecules on nanosheets. As shown in Figure 3b, the red glue can be painted on the glass substrate forming the solid red "HFNL" pattern further confirming the good adhesive capability of the Au NPs-chitosan-MTM red glue. More importantly, the Au NPs-chitosan-MTM hybrid nanosheets red glue can be easily dispersed into deionized water under ultrasonic action yielding a stable red suspension (Figure 4a). The UV−vis absorption spectra of these formed red Au NPs-chitosan-MTM hybrid nanosheet suspensions were collected (Figure 3c), which show the absorption peaks at 540 nm compared to that of chitosan-MTM hybrid nanosheets due to the surface plasmon resonance (SPR) band of Au NPs on hybrid nanosheets.[30,35,40] The well-defined shape of these Au NPs-chitosan-MTM hybrid nanosheet UV−vis spectra indicates the high dispersibility of these hybrid nanosheets as well. Additionally, the absorption intensity of Au NPs-chitosan-MTM hybrid nanosheets increased with the distribution density of Au NPs on chitosan-MTM hybrid nanosheets because of the stronger SPR effect induced by more Au NPs on the nanosheets.

Air Brush Assisted Assembly of Au NPs-Chitosan-MTM Nanosheets To Form Nacre-like Hybrid Coatings. The good dispersion of functional Au NPs-chitosan-MTM nanosheets in deionized water promoted feasible fabrication techniques to assemble these functional building blocks, forming nacre-like layered structures. Through

the airbrush assisted spraying technique, the synthesized Au NPs-chitosan-MTM nanosheets can homogeneously assemble on glass substrates and even polyethylene terephthalate (PET) films generating transparent nacre-like hybrid coatings. As shown in Figure S3, Au NPs-chitosan-MTM nanosheets colored glass substrates to red and the color became dark with the increase of the distribution density of Au NPs decorated on the MTM nanosheets. Spraying functional Au NPs-chitosan-MTM nanosheets on PET substrates lead to the formation of flexible transparent pink coatings, indicating the versatility of the obtained functional hybrid nanosheets (Figure 4b). The formation of the Au NPs-chitosan-MTM transparent homogeneous hybrid coatings on various substrates ascribed to highly oriented two-dimensional structures and strong adhesive properties of the obtained hybrid nanosheets. Under the influence of airbrush triggered air flow the Au NPs-chitosan-MTM hybrid nanosheets preferred to horizontally stack on the substrates with each other. With the evaporation of deionized water the chitosan molecules on MTM nanosheets acted as the glue that tightly sticks the hybrid nanosheets together. The cross section and surface microstructures of the Au NPs-chitosan-MTM hybrid coating on PET substrates were characterized by scanning electron microscopy (SEM) to confirm the formation of well-defined nacre-like layered structural hybrid coatings. As shown in Figure 4c, Au NPs-chitosan-MTM hybrid nanosheets arranged on the PET substrate layer by layer forming nacre-like lamellar microstructures. The surface SEM image of the Au NPs-chitosan-MTM hybrid nanosheets coating on PET (Figure 4d) indicates that hybrid nanosheets are almost flatly stacked and sandwiched by small Au NPs. These results demonstrate the feasibility and efficiency of the formation of the nacre-like hybrid coating *via* air brush spraying, using Au NPs-chitosan-MTM hybrid nanosheets as building blocks.

Optical, SERS, and Catalytic Properties of Au NPs-Chitosan-MTM Artificial Nacre Coatings. Because of the deposition of Au NPs with chitosan-MTM nanosheets and the uniform lamellar construction of hybrid nanosheets, the obtained coatings on substrates were colored by Au NPs and transparent as well. The optical properties of these Au NPs-chitosan-MTM hybrid coatings were revealed by UV−vis transmittance spectra. As shown in Figure 5a, the Au NPs-chitosan-MTM hybrid coatings (the thickness of these coatings is about 1.5 μm as shown in Figure 4c) behave with about 60−90% transparence across the visible spectrum of light and intensive absorptions at about 540 nm caused by the SPR of Au NPs in these hybrid coatings. Interestingly, due to the plasmon resonance of Au NPs embedded in coatings, the attractive surface enhanced Raman scattering (SERS) functionality for molecular sensing was introduced in these nacre-like hybrid coatings.[43−45] 4-Mercaptobenzoic acid (4-MBA) was used as the probe molecule for the SERS measurement to investigate the enhancement effect of the Au NPs-chitosan-MTM hybrid coating because of the good adsorption of 4-MBA on the surfaces of Au NPs. Figure 5b shows a series of SERS spectra of 4-MBA on different glass substrates at an excitation wavelength of 785 nm and with an acquisition time of 10 s. The SERS effect of the Au NPs-chitosan-MTM hybrid coating was directly confirmed by obvious Raman signals of 4-MBA molecules (ν(CC) ring-breathing modes (1036 cm^{-1}) and ν(CH) bending modes (1117 and 1152 cm^{-1})) that can be observed on glass substrates with Au NPs-chitosan-MTM hybrid coatings compared with that on the original glass substrate. Furthermore, the intensity of the typical Raman signal of the $\nu(CC)_{ring}$ ring-breathing modes (1036 cm^{-1}) enhanced correspondingly with the increase of the densities of Au NPs on chitosan-MTM nanosheets. With the concentration ratio of chloroauric acid and the chitosan-MTM hybrid nanosheets increased from 1:25 to 4:25 in the synthesis system, the obtained hybrid coating induced $\nu(CC)_{ring}$ ring-breathing mode (1036 cm^{-1}) signal intensities were enhanced nearly 5-fold. This intensive improvement of SERS signals is considered to be related to the increase of the active surface or "hot spot" with the Au NP density increase in hybrid coatings. These results indicate that our fabricated Au NPs-chitosan-MTM hybrid coatings would be potentially feasible SERS substrate materials due to their facile fabrication.

In addition, the Au NPs loading on the PET film with chitosan-MTM hybrid nanosheets could also endow these nacre-like hybrid coatings with catalytic properties such as catalytic reduction of *p*-nitrophenol.[46−48] As shown in Figure 5c top, after the bent Au NPs-chitosan-MTM-PET films ($C_{chloroauric\ \ acid}$: $C_{chitosan\text{-}MTM}$ =2:25, the calculated amount of Au NPs on the PET film was 0.072 mmol) were immersed into a yellow mixed solution of *p*-nitrophenol and $NaBH_4$ for 3 min, the solution in contact with the Au NPs-chitosan-MTM hybrid coating became colorless. In contrast, the solution on the other side was still yellow. The color fade of the solution on the side of the Au NPs-chitosan-MTM hybrid coating indicated the highly catalytic role of the Au NPs-chitosan-MTM hybrid coating on the reduction of the *p*-nitrophenol by $NaBH_4$. The reduction of *p*-nitrophenol was further revealed by UV−vis absorption spectra. As shown in Figure 5d, the absorption of *p*-nitrophenol at 400 nm decreases with a prolonged reaction time; meanwhile, a new peak appears at 295 nm and gradually increases, indicating the reduction of *p*-nitrophenol to form *p*-aminophenol. The turnover number of the Au NPs-chitosan-MTM hybrid coating to *p*-nitrophenol was calculated as 690 based on the concentration variation determined by UV−vis spectra. More attractively, the Au NPs-chitosan-MTM hybrid coating was tightly attached to the PET film

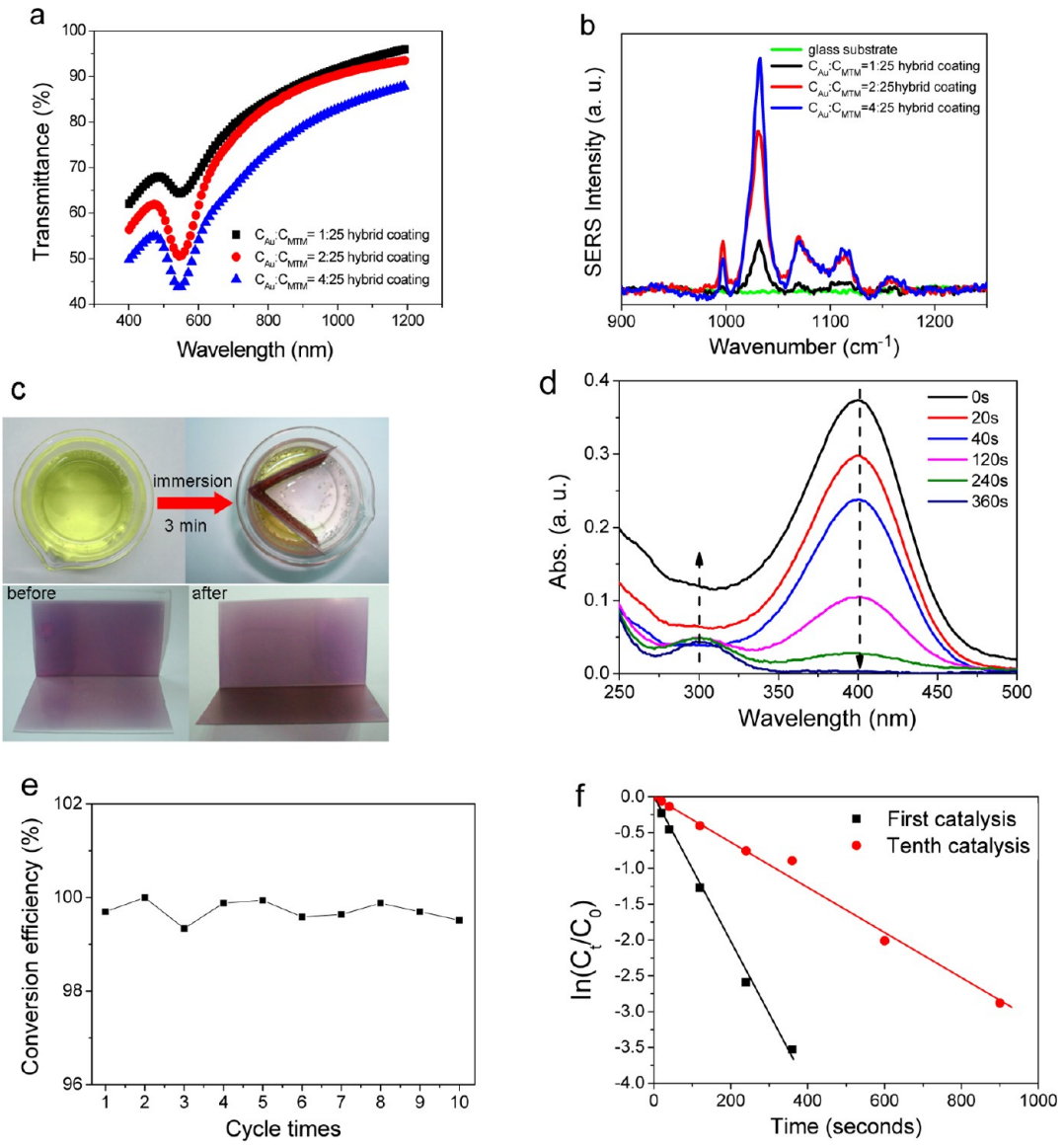

Figure 5. (a) UV−vis transmittance spectra of Au NPs-chitosan-MTM hybrid coatings on glass substrates with different Au NP densities attached on hybrid nanosheets. The thickness of hybrid coatings on glass substrates was about 1.5 μm. (b) SERS spectra of 1 mM 4-MBA molecules collected on bare glass substrate and a set of Au NPs-chitosan-MTM hybrid coatings on glass substrates with different Au NPs densities attached on hybrid nanosheets. (c) Top: photographic illustration of the reduction of *p*-nitrophenol by $NaBH_4$ under catalysis of Au NPs-chitosan-MTM hybrid coating. Bottom: the photos of Au NPs-chitosan-MTM hybrid coating before and after as catalyst. (d) The reduction of *p*-nitrophenol in aqueous solution recorded at several intervals using Au NPs-chitosan-MTM hybrid coating on PET as a catalyst. (e) The reusability of the Au NPs-chitosan-MTM hybrid coating as a catalyst for the reduction of 4-nitrophenol by $NaBH_4$. (f) The relationship between $\ln(C_t/C_0)$ and reaction time (t), wherein C_t/C_0 values of 4-nitrophenol were directly given by the relative intensity of the respective absorbance A_t/A_0.

even under the flow of bubbling generated by the decomposition of $NaBH_4$ (Figure 5c bottom) implying the stabilization and cyclic capability of the Au NPs-chitosan-MTM hybrid coating. The reusability of the Au NPs-chitosan-MTM hybrid coating was investigated by repeated immersion in a freshly mixed solution of *p*-nitrophenol and $NaBH_4$. Figure 5e shows that the hybrid coating exhibited similar catalytic performance without a visible decrease in the conversion efficiency for the same reaction time (15 min) even after running for 10 cycles. The reaction rate of this reduction process was revealed by the linear relationship between $\ln(C_t/C_0)$ and reaction time (t) (Figure 5f), which matches with the first-order reaction kinetics because reductant concentration is much higher than that of *p*-nitrophenol ($C_{NaBH_4}/C_{nitrophenol}$ = 158). The rate constant k was calculated to be 9.9×10^{-3} and 3.1×10^{-3} s^{-1} for the first catalysis and tenth catalysis reactions, respectively, which indicates that the reaction rate decreased 3-fold after cyclic utilization 10 times.

Vacuum Filtration Assisted Self-Assembly To Form Free-Standing Nacre-like Hybrid Films. Besides the spray

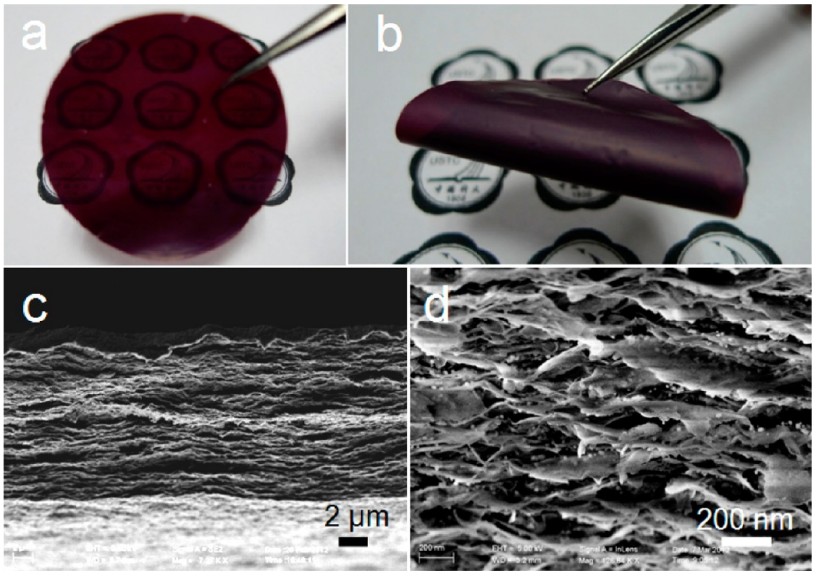

Figure 6. (a and b) Photographs of free-standing Au NPs-chitosan-MTM nacre-like functional hybrid films. (c) Cross section SEM image of Au NPs-chitosan-MTM nacre-like hybrid film. (d) Magnified cross section SEM image.

fabrication of Au NPs-chitosan-MTM nanosheet coatings on substrates, the highly dispersive Au NPs-chitosan-MTM hybrid nanosheets in deionized water can self-assemble to prepare free-standing nacre-like functional hybrid films *via* vacuum filtration as previously reported chitosan-MTM hybrid nanosheets.[22] As shown in Figure 6a and 6b, the fabricated Au NPs-chitosan-MTM hybrid films are freestanding, translucent, dark red, and flexible. The dark red colors of these hybrid films were caused by Au NPs attached to the hybrid nanosheets. The flexibility of these hybrid films was still maintained after embedding Au NPs. The cross section SEM image of Au NPs-chitosan-MTM hybrid films was shown in Figure 6c displaying the well-defined nacre-like lamellar structures induced by vacuum filtration assisted assembly of two-dimensional hybrid nanosheets. The higher magnification SEM image in Figure 6d further clearly shows that Au NPs were incorporated in lamellar structures and encapsulated by MTM nanosheets. Thus, the artificial nacre-like Au NP functionalized freestanding hybrid films can be produced in large scale *via* the present facile, green, and time-saving fabrication route.

Tensile Strength of Au NPs-Chitosan-MTM Artificial Nacre-like Hybrid Films. The tensile strength of these Au NPs-chitosan-MTM functional hybrid films was measured to investigate the influence of Au NP insertion on the mechanical properties of these nacre-like hybrid films. The stress–strain curves were plotted in Figure 7 showing that with increasing the amount of Au NPs grown on the chitosan-MTM nanosheets, the ultimate tensile strength of hybrid films decreased from 85 to 18 MPa. The Young modulus of these hybrid films also decreased (from 5 to 1 GPa) with the increased amount of Au NPs incorporated in the layered structures. The deterioration of mechanical properties of the obtained

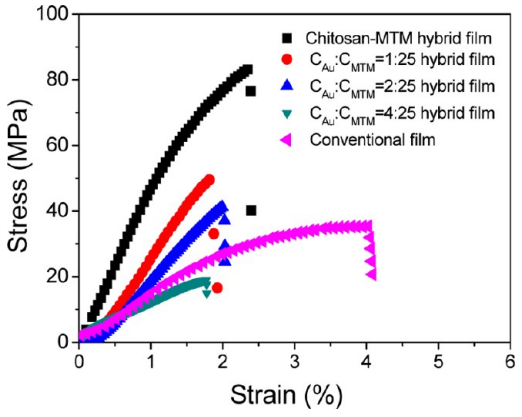

Figure 7. Tensile stress–strain curves of various chitosan-MTM hybrid films and Au NPs-chitosan-MTM hybrid films with different concentrations of Au NPs.

Au NPs-chitosan-MTM hybrid films with the incorporation of Au NPs was attributed to the weakened adhesive forces of Au nanoparticle interfaces compared with the hydrogen bonding of chitosan molecules. It is worth noting that the tensile strength of Au NPs-chitosan-MTM hybrid films is still higher or comparable to that of conventional film made by randomly mixing chitosan and MTM.[22] The maintenance of the Au NPs-chitosan-MTM hybrid films' tensile strength at a relatively high level indicates the contribution of nacre-like layered structures on the enhancement of mechanical properties as well.

Photothermal Activities of Au NPs-Chitosan-MTM Artificial Nacre-like Hybrid Films. The optical properties of Au NPs-chitosan-MTM hybrid films were revealed by UV–vis absorption spectra (Figure S4), indicating the strong absorption across the visible light and near-infrared spectrum due to the SPR and coupling of Au NPs encapsulated between nanosheets. The absorbed light

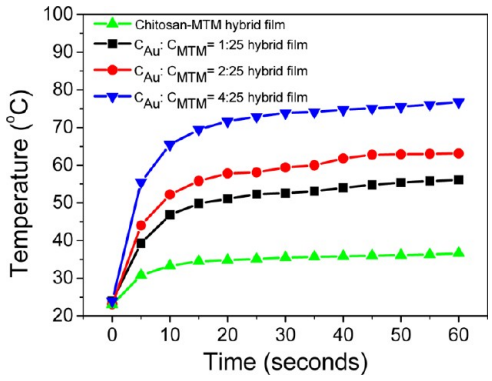

Figure 8. Temperature rise traces of thermal probes attached with different hybrid films under irradiation of an 808 nm infrared diode laser with a power density of 8 W·cm^{-2}.

would further convert to heat nearly completely by Au NPs which is well-known as the photothermal conversion effect. The fundamental aspects of the photothermal conversion caused by the localized plasmon resonances of Au NPs have been comprehensively studied.[49−51] The plasmonic photothermal conversion effect of Au NPs has been shown for various applications, such as photothermal imaging,[52] cancer therapy,[53,54] and gene delivery.[55] Here, we investigated the photothermal conversion effect of free-standing Au NPs-chitosan-MTM hybrid films to further demonstrate the functionalities and potential applications of our fabricated nacre-like Au NPs-chitosan-MTM hybrid films. The freestanding Au NPs-chitosan-MTM hybrid films were cut into pieces ~0.5 cm × 1 cm in size and then attached onto the thermal probe. A 808 nm infrared diode laser with a power density of 8 W·cm^{-2} was used as the light source to irradiate the Au NPs-chitosan-MTM hybrid films. The heat generated by the Au NPs-chitosan-MTM hybrid films was detected by the thermal probe. The temperature variation of the thermal probe with the irradiation time prolonged was recorded and plotted. As shown in Figure 8, Au NPs-chitosan-MTM hybrid films induced an obviously quicker temperature increase of the thermal probes *via* the photothermal conversion effect than chitosan-MTM hybrid films, indicating their photothermal conversion functionality endowed by Au NPs. Moreover, the hybrid film triggered a rise in temperature rate, and the ultimate temperatures of the heating targets increased with the number of Au NPs on chitosan-MTM hybrid nanosheets. The ultimate temperatures of the objects heated by Au NPs-chitosan-MTM hybrid films made by concentration ratios of chloroauric acid and the chitosan-MTM hybrid nanosheets in the reaction system of 1:25, 2:25, and 4:25 can reach 54, 63, and 79 °C, respectively (Figure S5). The rapid temperature rise and relatively high ultimate temperatures generated by the photothermal conversion effect of the Au NPs-chitosan-MTM hybrid films implied their potential applications as heating sources for microdevices[56] and as photothermal therapy membranes,[57] to name a few.

CONCLUSION

In summary, we report a feasible route to fabricate multifunctional artificial nacre-like hybrid films by using Au NP modified MTM nanosheets as efficient two-dimensional building blocks. Through the facile *in situ* growth of Au NPs on chitosan-MTM nanosheets, Au NPs-chitosan-MTM hybrid nanosheets can be prepared and homogeneously dispersed in deionized water. The aqueous suspension of Au NPs-chitosan-MTM hybrid nanosheets can be feasibly sprayed and vacuum filtrated to form nacre-like layered hybrid nanocoatings and free-standing hybrid films, respectively. The fabricated Au NPs-chitosan-MTM hybrid coatings were demonstrated as SERS and catalytic substrate materials, indicating the efficient functionalization of Au NPs to lamellar hybrid coatings. Moreover, free-standing Au NPs-chitosan-MTM layered structural hybrid films possess relatively high tensile strength and good photothermal conversion, implying their potential application as optical heating sources and photothermal therapy membranes. This facile and large scale fabrication of multifunctional Au NPs-chitosan-MTM nacre-like hybrid materials not only satisfies requirements for practical applications but also implicates an alternative route to functionalize nacre-like artificial hybrid materials.

METHODS

Materials. Sodium montmorillonite (Na-MTM) nanoclays were offered by Zhejiang Fenghong Clay Co. Ltd. Chitosan (≥90% deacetylated), glacial acetic acid, chloroauric acid tetrahydrate, sodium citrate dihydrate, *p*-nitrophenol, sodium borohydride, and 4-mercaptobenzoic acid were purchased from Sinopharm Chemical Reagent Co. Ltd. All reagents were analytical grade and used as received.

Chitosan-MTM Gel. Chitosan-MTM gel was prepared as we described before.[22] Typically, 1 g of MTM was dispersed in 200 mL of deionized water under vigorous stirring for 1 week, the solution was allowed to stand overnight, and the supernatant was collected as an MTM nanosheet solution for further use. 200 mL of 2 wt % chitosan (2 wt % of chitosan were prepared by dissolving chitosan in an aqueous solution of 2 wt % glacial acetic acid for 24 h before use) were added dropwise into the as-prepared MTM nanosheet solution and stirred for 20 h to form chitosan-MTM hybrid nanosheet sol. The sol was centrifuged (6000 rpm by 10 min) and washed with deionized water (DIW) one time, and then the obtained gel was redispersed into 200 mL of DIW. With the assumption that Na-MTM clays were fully exfoliated and all the chitosan molecules

absorbed on the MTM nanosheets, the concentration of chitosan-MTM in the as-prepared suspension was determined as 25 mg/mL.

Au NPs-Chitosan-MTM Hybrid Nanosheets Synthesis. A 30 mL aliquot of the above chitosan-MTM hybrid nanosheets suspension (25 mg/mL) was transferred into a flask containing 114 mL of boiled DIW heated to 115 °C by an oil bath under stirring, and then 3 mL of 10 mg/mL chloroauric acid ($HAuCl_4$) were added into the flask. The solution continued to reflux and stir for 3 min to ensure the $AuCl_4^-$ ions adsorb onto nanosheets. Then, 3 mL (equal volume to chloroauric acid) of 20 mg/mL sodium citrate solution were dropped into the flask. The total volume of the mixture was 150 mL, and the concentrations of chitosan-MTM, $HAuCl_4$, and sodium citrate were 5, 0.2, and 0.4 mg/mL, respectively. The obtained suspension was refluxed at 115 °C for 3 min to yield red floccules in suspension. Several drops of the obtained red suspension were taken out for TEM characterization. The final red floccules were collected by centrifugation (2000 rpm, 10 min) as adhesive red glue. To increase the distribution density of gold nanoparticles decorating the chitosan-MTM nanosheets, the concentration of the chitosan-MTM hybrid nanosheets in the synthetic process was decreased to 2.5 and 1.25 mg/mL, respectively, and the other conditions were kept constant. The obtained red Au NPs-chitosan-MTM hybrid nanosheet glue was redispersed in 30, 15, and 7.5 mL of 5 wt % acetic acid by stirring and ultrasonication, respectively, for further self-assembly to form nacre-like hybrid coatings and freestanding films.

Control Synthesis of Au NPs-Chitosan-MTM Hybrid Nanosheets without Adding Sodium Citrate. A 30 mL aliquot of the chitosan-MTM hybrid nanosheets suspension (25 mg/mL) was added into a flask containing 117 mL of boiled DIW heated to 115 °C by an oil bath under stirring, and then 3 mL of 10 mg/mL chloroauric acid ($HAuCl_4$) were added into the flask. The obtained suspension was refluxed at 115 °C for 30 min to gain a stable red suspension. Several drops of this red suspension were taken out for further TEM characterization.

Spray Coating on Glass and PET Membrane. Both substrates were cleaned with DIW and ethanol before use. The pressure of the air compressor was 0.4 MPa. The Au NP modified nanosheet suspension (15 mL) was poured into an air brush. The substrate was heated to 90 °C by a heating plate, and the suspension was atomized and sprayed onto the surface of the substrate at an appropriate solution flow rate (~5 mL/min) and spray distance (~10 cm).

Freestanding Au NPs-Chitosan-MTM Hybrid Film Preparation. A 10 mL aliquot of the Au NPs-chitosan-MTM nanosheet suspension was filtrated by a cellulose acetate filter membrane (pore diameter 0.22 μm) set on a sand core funnel. The wet hybrid film was rinsed gently with DIW and dried by nitrogen flow. Consequently, the film can be easily peeled off from the filter membrane.

Characterization. TEM images were acquired with a Hitachi H-7650 transmission electron microscope at an acceleration voltage of 120 kV. SEM images were acquired with a Zeiss Supra 40 scanning electron microscope at an acceleration voltage of 5 kV. The UV−vis transmittance and adsorption spectra of the films were collected on a SHIMADZU DUV-3700. The UV−vis adsorption spectra of suspensions were recorded by a Shimadzu UV-2500 PC. The suspension for UV−vis spectra analysis was diluted to one-tenth of the original concentration with DIW. The mechanical properties of freestanding films were measured under tensile mode in a universal mechanical testing machine (Instron 5565 A). For the mechanical - testing, the films were cut with a razor blade into rectangle bars of approximate length 15 mm and width 5 mm; the distance between the clamps was 5 mm, and the load speed was 10 mm/min. Raman scattering spectra were measured using a confocal Raman microscope (LabRAM HR, HORIBA Jobin Yvon Inc.) with an excitation wavelength of 785 nm. Photothermal conversion properties were tested with a 808 nm infrared diode laser with a power density of 8 $W \cdot cm^{-2}$ (Changchun New Industries Optoelectronics Technology Co., Ltd.) and a thermometer (TES-1310, TES Electrical Electronic Corp.).

Recyclable Catalysis of *p*-Nitrophenol by Au NPs-Chitosan-MTM Coated PET Membrane. Typically, 30 mL of newly prepared 0.264 M sodium borohydride and 20 mL of 2.5 mM *p*-nitrophenol were mixed together in a beaker. The beaker was kept in a 45 °C oven for 10 min, and then a piece of Au NPs-chitosan-MTM nanosheet coated PET membrane was immersed into the solution for 15 min and 0.5 mL of the solution was extracted for further UV−vis absorption analysis at certain intervals. The membrane was then taken out from solution and gently rinsed with DIW. The above process was repeated 10 times to investigate the recycled efficiency of the hybrid coating as the catalyst.

SERS Sample Preparation. SERS substrates were prepared by spraying 10 mL of the as-prepared nanosheet suspensions onto glass slide (25 mm × 76 mm), and then small pieces of the slide were cut and immersed into 4 mL of 0.5 mM 4-mercaptobenzoic acid in ethanol for 5 h and then washed with ethanol and dried at room temperature.

Conflict of Interest: The authors declare no competing financial interest.

Acknowledgment. This work is supported by the National Basic Research Program of China (Grant 2010CB934700), the National Natural Science Foundation of China (Grant Nos. 91022032, 21061160492, J1030412), the Chinese Academy of Sciences (Grant KJZD-EW-M01-1), the International Science & Technology Cooperation Program of China (Grant 2010DFA41170), and the Principal Investigator Award by the National Synchrotron Radiation Laboratory at the University of Science and Technology of China.

Supporting Information Available: SEM images, TEM images, photographs, and UV−vis adsorption spectra. This material is available free of charge *via* the Internet at http://pubs.acs.org.

REFERENCES AND NOTES

1. Fratzl, P.; Weinkamer, R. Nature's Hierarchical Materials. *Prog. Mater. Sci.* **2007**, *52*, 1263–1334.
2. Meyers, M. A.; Chen, P.-Y.; Lin, A. Y.-M.; Seki, Y. Biological Materials: Structure and Mechanical Properties. *Prog. Mater. Sci.* **2008**, *53*, 1–206.
3. Jackson, A. P.; Vincent, J. F. V.; Turner, R. M. The Mechanical Design of Nacre. *Proc. R. Soc. London, Ser. B* **1988**, *234*, 415–440.
4. Luz, G. M.; Mano, J. F. Biomimetic Design of Materials and Biomaterials Inspired by the Structure of Nacre. *Philos. Trans. R. Soc. London, Ser. A* **2009**, *367*, 1587–1605.
5. Bhushan, B. Biomimetics: Lessons from Nature - An Overview. *Philos. Trans. R. Soc. London, Ser. A* **2009**, *367*, 1445–1486.
6. Mayer, G. New Classes of Tough Composite Materials--Lessons from Natural Rigid Biological Systems. *Mater. Sci. Eng., C* **2006**, *26*, 1261–1268.
7. Li, X.; Chang, W.-C.; Chao, Y. J.; Wang, R.; Chang, M. Nanoscale Structural and Mechanical Characterization of a Natural Nanocomposite Material: The Shell of Red Abalone. *Nano Lett.* **2004**, *4*, 613–617.
8. Song, F.; Soh, A. K.; Bai, Y. L. Structural and Mechanical Properties of the Organic Matrix Layers of Nacre. *Biomaterials* **2003**, *24*, 3623–3631.
9. Wang, J.; Cheng, Q.; Tang, Z. Layered Nanocomposites Inspired by the Structure and Mechanical Properties of Nacre. *Chem. Soc. Rev.* **2012**, *41*, 1111–1129.
10. Yao, H.-B.; Fang, H.-Y.; Wang, X.-H.; Yu, S.-H. Hierarchical Assembly of Micro-/Nano-Building Blocks: Bio-Inspired Rigid Structural Functional Materials. *Chem. Soc. Rev.* **2011**, *40*, 3764–3785.
11. Tang, Z.; Kotov, N. A.; Magonov, S.; Ozturk, B. Nanostructured Artificial Nacre. *Nat. Mater.* **2003**, *2*, 413–418.
12. Munch, E.; Launey, M. E.; Alsem, D. H.; Saiz, E.; Tomsia, A. P.; Ritchie, R. O. Tough, Bio-Inspired Hybrid Materials. *Science* **2008**, *322*, 1516–1520.
13. Yao, H.-B.; Fang, H.-Y.; Tan, Z.-H.; Wu, L.-H.; Yu, S.-H. Biologically Inspired, Strong, Transparent, and Functional Layered Organic-Inorganic Hybrid Films. *Angew. Chem., Int. Ed.* **2010**, *49*, 2140–2145.

14. Kato, T. Polymer/Calcium Carbonate Layered Thin-Film Composites. *Adv. Mater.* **2000**, *12*, 1543–1546.
15. Podsiadlo, P.; Kaushik, A. K.; Arruda, E. M.; Waas, A. M.; Shim, B. S.; Xu, J.; Nandivada, H.; Pumplin, B. G.; Lahann, J.; Ramamoorthy, A.; Kotov, N. A. Ultrastrong and Stiff Layered Polymer Nanocomposites. *Science* **2007**, *318*, 80–83.
16. Podsiadlo, P.; Shim, B. S.; Kotov, N. A. Polymer/Clay and Polymer/Carbon Nanotube Hybrid Organic-Inorganic Multilayered Composites Made by Sequential Layering of Nanometer Scale Films. *Coord. Chem. Rev.* **2009**, *253*, 2835–2851.
17. Long, B.; Wang, C.-A.; Lin, W.; Huang, Y.; Sun, J. Polyacrylamide-Clay Nacre-Like Nanocomposites Prepared by Electrophoretic Deposition. *Compos. Sci. Technol.* **2007**, *67*, 2770–2774.
18. Lin, W.; Wang, C.-a.; Le, H.; Long, B.; Huang, Y. Special Assembly of Laminated Nanocomposite That Mimics Nacre. *Mater. Sci. Eng., C* **2008**, *28*, 1031–1037.
19. Chen, R.; Wang, C.-A.; Huang, Y.; Le, H. An Efficient Biomimetic Process for Fabrication of Artificial Nacre with Ordered-Nanostructure. *Mater. Sci. Eng., C* **2008**, *28*, 218–222.
20. Walther, A.; Bjurhager, I.; Malho, J. M.; Ruokolainen, J.; Berglund, L.; Ikkala, O. Supramolecular Control of Stiffness and Strength in Lightweight High-Performance Nacre-Mimetic Paper with Fire-Shielding Properties. *Angew. Chem., Int. Ed.* **2010**, *49*, 6448–6453.
21. Walther, A.; Bjurhager, I.; Malho, J.-M.; Pere, J.; Ruokolainen, J.; Berglund, L. A.; Ikkala, O. Large-Area, Lightweight and Thick Biomimetic Composites with Superior Material Properties *via* Fast, Economic, and Green Pathways. *Nano Lett.* **2010**, *10*, 2742–2748.
22. Yao, H.-B.; Tan, Z.-H.; Fang, H.-Y.; Yu, S.-H. Artificial Nacre-like Bionanocomposite Films from the Self-Assembly of Chitosan−Montmorillonite Hybrid Building Blocks. *Angew. Chem., Int. Ed.* **2010**, *49*, 10127–10131.
23. Ebina, T.; Mizukami, F. Flexible Transparent Clay Films with Heat-Resistant and High Gas-Barrier Properties. *Adv. Mater.* **2007**, *19*, 2450–2453.
24. Priolo, M. A.; Gamboa, D.; Holder, K. M.; Grunlan, J. C. Super Gas Barrier of Transparent Polymer−Clay Multilayer Ultrathin Films. *Nano Lett.* **2010**, *10*, 4970–4974.
25. Srivastava, S.; Kotov, N. A. Composite Layer-by-Layer (LBL) Assembly with Inorganic Nanoparticles and Nanowires. *Acc. Chem. Res.* **2008**, *41*, 1831–1841.
26. Mamedov, A.; Ostrander, J.; Aliev, F.; Kotov, N. A. Stratified Assemblies of Magnetite Nanoparticles and Montmorillonite Prepared by the Layer-by-Layer Assembly. *Langmuir* **2000**, *16*, 3941–3949.
27. Lee, B.; Kim, Y.; Lee, S.; Kim, Y. S.; Wang, D.; Cho, J. Layer-by-Layer Growth of Polymer/Quantum Dot Composite Multilayers by Nucleophilic Substitution in Organic Media. *Angew. Chem., Int. Ed.* **2010**, *49*, 359–363.
28. Sakai, N.; Sasaki, T.; Matsubara, K.; Tatsuma, T. Layer-by-Layer Assembly of Gold Nanoparticles with Ttitania Nanosheets: Control of Plasmon Resonance and Photovoltaic Properties. *J. Mater. Chem.* **2010**, *20*, 4371–4378.
29. Yao, H.-B.; Wu, L.-H.; Cui, C.-H.; Fang, H.-Y.; Yu, S.-H. Direct Fabrication of Photoconductive Patterns on LBL Assembled Graphene Oxide/PDDA/Titania Hybrid Films by Photothermal and Photocatalytic Reduction. *J. Mater. Chem.* **2010**, *20*, 5190–5195.
30. Daniel, M.-C.; Astruc, D. Gold Nanoparticles: Assembly, Supramolecular Chemistry, Quantum-Size-Related Properties, and Applications toward Biology, Catalysis, and Nanotechnology. *Chem. Rev.* **2003**, *104*, 293–346.
31. Jiang, C.; Markutsya, S.; Pikus, Y.; Tsukruk, V. V. Freely Suspended Nanocomposite Membranes as Highly Sensitive Sensors. *Nat. Mater.* **2004**, *3*, 721–728.
32. Elghanian, R.; Storhoff, J. J.; Mucic, R. C.; Letsinger, R. L.; Mirkin, C. A. Selective Colorimetric Detection of Polynucleotides Based on the Distance-Dependent Optical Properties of Gold Nanoparticles. *Science* **1997**, *277*, 1078–1081.
33. Jiang, C.; Markutsya, S.; Tsukruk, V. V. Compliant, Robust, and Truly Nanoscale Free-Standing Multilayer Films Fabricated Using Spin-Assisted Layer-by-Layer Assembly. *Adv. Mater.* **2004**, *16*, 157–161.
34. Jiang, C.; McConney, M. E.; Singamaneni, S.; Merrick, E.; Chen, Y.; Zhao, J.; Zhang, L.; Tsukruk, V. V. Thermo-Optical Arrays of Flexible Nanoscale Nanomembranes Freely Suspended over Microfabricated Cavities as IR Microimagers. *Chem. Mater.* **2006**, *18*, 2632–2634.
35. Lu, C.; Dönch, I.; Nolte, M.; Fery, A. Au Nanoparticle-based Multilayer Ultrathin Films with Covalently Linked Nanostructures: Spraying Layer-by-layer Assembly and Mechanical Property Characterization. *Chem. Mater.* **2006**, *18*, 6204–6210.
36. Huang, H.; Yang, X. Synthesis of Chitosan-Stabilized Gold Nanoparticles in the Absence/Presence of Tripolyphosphate. *Biomacromolecules* **2004**, *5*, 2340–2346.
37. Wang, B.; Chen, K.; Jiang, S.; Reincke, F.; Tong, W.; Wang, D.; Gao, C. Chitosan-Mediated Synthesis of Gold Nanoparticles on Patterned Poly(dimethylsiloxane) Surfaces. *Biomacromolecules* **2006**, *7*, 1203–1209.
38. Bhumkar, D.; Joshi, H.; Sastry, M.; Pokharkar, V. Chitosan Reduced Gold Nanoparticles as Novel Carriers for Transmucosal Delivery of Insulin. *Pharm. Res.* **2007**, *24*, 1415–1426.
39. Nivedita, B.; Resham, B.; Priyabrata, M. Protein-Mediated Autoreduction of Gold Salts to Gold Nanoparticles. *Biomed. Mater.* **2008**, *3*, 034105.
40. Das, S. K.; Dickinson, C.; Lafir, F.; Brougham, D. F.; Marsili, E. Synthesis, Characterization and Catalytic Activity of Gold Nanoparticles Biosynthesized with Rhizopus Oryzae Protein Extract. *Green Chem.* **2012**, *14*, 1322–1334.
41. Engelbrekt, C.; Sorensen, K. H.; Zhang, J.; Welinder, A. C.; Jensen, P. S.; Ulstrup, J. Green Synthesis of Gold Nanoparticles with Starch-Glucose and Application in Bioelectrochemistry. *J. Mater. Chem.* **2009**, *19*, 7839–7847.
42. Genç, R. K.; Clergeaud, G.; Ortiz, M.; O'Sullivan, C. K. Green Synthesis of Gold Nanoparticles Using Glycerol-Incorporated Nanosized Liposomes. *Langmuir* **2011**, *27*, 10894–10900.
43. Doering, W. E.; Piotti, M. E.; Natan, M. J.; Freeman, R. G. SERS as a Foundation for Nanoscale, Optically Detected Biological Labels. *Adv. Mater.* **2007**, *19*, 3100–3108.
44. Talley, C. E.; Jackson, J. B.; Oubre, C.; Grady, N. K.; Hollars, C. W.; Lane, S. M.; Huser, T. R.; Nordlander, P.; Halas, N. J. Surface-Enhanced Raman Scattering from Individual Au Nanoparticles and Nanoparticle Dimer Substrates. *Nano Lett.* **2005**, *5*, 1569–1574.
45. Li, J. F.; Huang, Y. F.; Ding, Y.; Yang, Z. L.; Li, S. B.; Zhou, X. S.; Fan, F. R.; Zhang, W.; Zhou, Z. Y.; WuDe, Y.; Ren, B.; Wang, Z. L.; Tian, Z. Q. Shell-Isolated Nanoparticle-Enhanced Raman Spectroscopy. *Nature* **2010**, *464*, 392–395.
46. Lee, J.; Park, J. C.; Song, H. A Nanoreactor Framework of a $Au@SiO_2$ Yolk/Shell Structure for Catalytic Reduction of *p*-Nitrophenol. *Adv. Mater.* **2008**, *20*, 1523–1528.
47. Deng, Y.; Cai, Y.; Sun, Z.; Liu, J.; Liu, C.; Wei, J.; Li, W.; Liu, C.; Wang, Y.; Zhao, D. Multifunctional Mesoporous Composite Microspheres with Well-Designed Nanostructure: A Highly Integrated Catalyst System. *J. Am. Chem. Soc.* **2010**, *132*, 8466–8473.
48. Zeng, J.; Zhang, Q.; Chen, J.; Xia, Y. A Comparison Study of the Catalytic Properties of Au-Based Nanocages, Nanoboxes, and Nanoparticles. *Nano Lett.* **2009**, *10*, 30–35.
49. Jain, P. K.; Huang, X.; El-Sayed, I. H.; El-Sayed, M. A. Noble Metals on the Nanoscale: Optical and Photothermal Properties and Some Applications in Imaging, Sensing, Biology, and Medicine. *Acc. Chem. Res.* **2008**, *41*, 1578–1586.
50. Richardson, H. H.; Carlson, M. T.; Tandler, P. J.; Hernandez, P.; Govorov, A. O. Experimental and Theoretical Studies of Light-to-Heat Conversion and Collective Heating Effects in Metal Nanoparticle Solutions. *Nano Lett.* **2009**, *9*, 1139–1146.
51. Chen, H.; Shao, L.; Ming, T.; Sun, Z.; Zhao, C.; Yang, B.; Wang, J. Understanding the Photothermal Conversion Efficiency of Gold Nanocrystals. *Small* **2010**, *6*, 2272–2280.

52. Boyer, D.; Tamarat, P.; Maali, A.; Lounis, B.; Orrit, M. Photothermal Imaging of Nanometer-Sized Metal Particles Among Scatterers. *Science* **2002**, *297*, 1160–1163.
53. Lal, S.; Clare, S. E.; Halas, N. J. Nanoshell-Enabled Photothermal Cancer Therapy: Impending Clinical Impact. *Acc. Chem. Res.* **2008**, *41*, 1842–1851.
54. Skrabalak, S. E.; Chen, J.; Sun, Y.; Lu, X.; Au, L.; Cobley, C. M.; Xia, Y. Gold Nanocages: Synthesis, Properties, and Applications. *Acc. Chem. Res.* **2008**, *41*, 1587–1595.
55. Lee, S. E.; Liu, G. L.; Kim, F.; Lee, L. P. Remote Optical Switch for Localized and Selective Control of Gene Interference. *Nano Lett.* **2009**, *9*, 562–570.
56. Fang, C.; Shao, L.; Zhao, Y.; Wang, J.; Wu, H. A Gold Nanocrystal/Poly(dimethylsiloxane) Composite for Plasmonic Heating on Microfluidic Chips. *Adv. Mater.* **2012**, *24*, 94–98.
57. Huang, X.; Jain, P.; El-Sayed, I.; El-Sayed, M. Plasmonic Photothermal Therapy (PPTT) Using Gold Nanoparticles. *Lasers Med. Sci.* **2008**, *23*, 217–228.